THE FASEB JOURNAL • RESEARCH • www.fasebj.org

Platelet-derived microparticles promote endothelial cell proliferation in hypertension *via* miR-142-3p

Han Bao, Yuan-Xiu Chen, Kai Huang, Fei Zhuang, Min Bao, Yue Han, Xiao-Hu Chen, Qian Shi, Qing-Ping Yao,[1] and Ying-Xin Qi[2]

Institute of Mechanobiology and Medical Engineering, School of Life Sciences and Biotechnology, Shanghai Jiao Tong University, Shanghai, China

ABSTRACT: Endothelial cells (ECs) are located at the interface between flowing blood and the vessel wall, and abnormal EC proliferation induced by pathologic environments plays an important role in vascular remodeling in hypertensive conditions. Exchanges of information between blood components and ECs are important for EC function. Hence, the present study sought to determine how platelets induce EC dysfunction under hypertensive conditions. EC proliferation was increased in renal hypertensive rats established by abdominal aortic coarctation compared with control rats and that elevated thrombin in plasma promoted platelet activation, which may induce the release of platelet-derived microparticles (PMPs). MicroRNA (MiR) array and qPCR revealed a higher level of miR-142-3p in platelets and PMPs. *In vitro*, PMPs delivered miR-142-3p into ECs and enhanced their proliferation *via* Bcl-2-associated transcription factor (BCLAF)1 and its downstream genes. These results indicate that PMPs deliver miR-142-3p from activated platelets into ECs and that miR-142-3p may play important roles in EC dysfunction in hypertensive conditions and may be a novel therapeutic target for maintaining EC homeostasis in hypertension.—Bao, H., Chen, Y.-X., Huang, K., Zhuang, F., Bao, M., Han, Y., Chen, X.-H., Shi, Q., Yao, Q.-P., Qi, Y.-X. Platelet-derived microparticles promote endothelial cell proliferation in hypertension *via* miR-142-3p. FASEB J. 32, 3912–3923 (2018). www.fasebj.org

KEY WORDS: intercellular communication · microRNA · vascular homeostasis · BCLAF1

Endothelial cells (ECs), which are located at the interface between flowing blood and the vessel wall, serve as a semipermeable barrier and play critical roles in the maintenance of vascular physiologic functions. During homeostasis, the proliferative rate of mature ECs is relatively low (1). However, pathologic environments, such as hypertension, cause abnormal EC proliferation and other dysfunctions of ECs, thereby contributing to vascular remodeling (2). Interactions between many types of cells and ECs have been shown to be involved in many pathologic processes. For example, circulating monocytic cells secrete VEGF to promote EC proliferation, migration, and stability in acute lung injury (3). In addition, in thrombosis, activated platelets induced by thrombin adhere to ECs *via* several receptors, leading to EC activation and fibrin generation (4). In addition, platelets can be phagocytosed by ECs, and the phagocytosed platelets suppress EC apoptosis and promote cell viability (5). Although evidence shows that platelets play important roles in both EC homeostasis and dysfunction, the molecular mechanisms underlying how activated platelets modulate EC proliferation in hypertension remain unclear.

Microparticles (MPs) are extracellular vesicles ranging from 0.1 to 1 μm in size and have been shown to deliver various bioactive molecules [*i.e.*, chemokines (6), enzymes (7), and miRs (8)] to recipient cells. Increasing evidence shows that MPs play a pivotal role in many pathologic processes, such as cancer (9), inflammatory diseases (10), and cardiovascular disease (11). In the circulatory system, MPs are derived from their maternal cells, including ECs, vascular smooth muscle cells, erythrocytes, leukocytes, and platelets. In hypertension, activated platelets contribute the largest number of MPs to circulation, and chronic elevation of platelet-derived MPs (PMPs) correlates with the development of severe hypertension, which suggests that the number of PMPs is a potential biomarker of severe

ABBREVIATIONS: Bax, B-cell lymphoma-2–associated X protein; BCL2, B-cell lymphoma-2; BCLAF, Bcl-2–associated transcription factor; BrdU, bromodeoxyuridine; *cel-miR-39*, *Caenorhabditis elegans* miR-39; DBP, diastolic blood pressure; EC, endothelial cell; IPA, Ingenuity Pathway Analysis; LSE, laser scattering electrophoresis; miR, microRNA; MP, microparticles; PMP, platelet-derived microparticle; qPCR, quantitative PCR; SBP, systolic blood pressure; SSC, saline sodium citrate

[1] Correspondence: Institute of Mechanobiology and Medical Engineering, School of Life Sciences and Biotechnology, Shanghai Jiao Tong University, 800 Dongchuan Rd., P.O. Box 888, Minhang, Shanghai 200240, China. E-mail: qpyao@sjtu.edu.cn

[2] Correspondence: Institute of Mechanobiology and Medical Engineering, School of Life Sciences and Biotechnology, Shanghai Jiao Tong University, 800 Dongchuan Rd., P.O. Box 888, Minhang, Shanghai 200240, China. E-mail: qiyx@sjtu.edu.cn

doi: 10.1096/fj.201701073R

This article includes supplemental data. Please visit *http://www.fasebj.org* to obtain this information.

0892-6638/18/0032-3912 © FASEB

hypertension (12). In addition, the components of PMPs derived from hypertension-activated platelets are selected packaging that represents the modulating information. In the past decade, abundant proteins and miRs have been shown to be the major contents of PMPs. Recent research has shown that PMPs deliver miR-223 to ECs and repress the expression of target mRNAs (*i.e.*, f-box/WD repeat–containing protein-7 and ephrin-A1) (8). However, the roles of miRs delivered by PMPs in modulating EC function in hypertension are still not clear.

In the present study, we detected the role of PMPs in regulating EC proliferation in hypertension and further studied the effect of delivering miR-142-3p *via* PMPs. The study may provide new insight into the mechanism of EC dysfunction in hypertension and may provide novel targets for the maintenance of EC homeostasis.

MATERIALS AND METHODS

Hypertensive rat model and cell culture

The animal care and experimental protocols were in accordance with the Animal Management Rules of China (55, 2001, Ministry of Health, China), and the study was approved by the Animal Research Committee of Shanghai Jiao Tong University.

Renal hypertensive rats were generated by abdominal aortic coarctation (13). Male Sprague-Dawley rats with an average weight of 200 g were randomly assigned to the abdominal aorta–constriction group and sham-surgery control group. All animals were anesthetized with isoflurane inhalation and treated in sterile conditions. The abdomen was opened, and the abdominal aorta was surgically dissected from the inferior vena cava at a site just above the renal arteries. A 0.8 mm blunt needle was then placed along the side of the isolated aorta segment. Thereafter, a 3-0 suture was tightly tied around the aorta and the overlying needle. The needle was then removed, thus producing aortic constriction above the renal arteries. Animals assigned to the control group underwent the same procedure, but without actual ligation of the aorta.

The animals were then observed for 1 wk. Before the samples were harvested, blood pressure was measured directly *via* a carotid cannula method (13, 14). The animals were anesthetized with isoflurane, and the left carotid artery was catheterized with a 1.1 mm indwelling needle. Blood pressure was monitored directly *via* the arterial intubation which was connected to a multiple-lead physiologic recorder (MP30; Biopac Systems, Goleta, CA, USA).

Primary rat aortic ECs were obtained by digestion (15). ECs at passages 2–4 were used.

Preparation of platelets, circulating MPs, MP-poor plasma, and PMPs

Whole blood was collected from the abdominal aorta of anesthetized rats into syringes containing 100 μl/ml anticoagulant [2.94% sodium citrate, 136 mM glucose (pH 6.4), 0.1 g/ml PGE_1, and 1 U/ml apyrase], and the platelet-rich plasma was obtained by centrifuging at 1100 *g* for 10 min. Washed platelets were prepared from the platelet-rich plasma containing 5 mM EDTA by centrifuging at 2100 *g* for 10 min. The platelets were resuspended in modified Tyrode solution [12 mM $NaHCO_3$, 138 mM NaCl, 5.5 mM glucose, 2.9 mM KCl, 2 mM $MgCl_2$, 0.42 mM NaH_2PO_4, and 10 mM 4-(2-hydroxyethyl)-1-piperazineethanesulfonic acid (pH 7.4)]. After the platelets were collected, the remaining platelet-poor plasma was centrifuged at 20,500 *g* for 90 min to obtain circulating MPs and MP-poor plasma and the MPs were resuspended in 4-(2-hydroxyethyl)-1-piperazineethanesulfonic acid–Tyrode buffer.

Platelets were activated with 0.1 U/ml thrombin for 1 h and centrifuged at 2100 *g* for 10 min. PMPs were collected from the remaining supernatant using the methods described above for obtaining MPs. The control PMPs were isolated from the same amount of nonactivated platelets (16).

Flow cytometry and laser scattering electrophoresis and Brownian motion video microscopy

Platelets were analyzed by flow cytometry to determine their activation status. Platelets were labeled with FITC anti-Mouse/Rat CD61 (platelet marker, 1:100; Thermo Fisher Scientific, Waltham, MA, USA) and PE anti-mouse/rat CD62P (platelet activation marker, 1:100; BioLegend, San Diego, CA, USA) for 1 h and then loaded into a flow cytometry column. (FACSCalibur TM; BD Biosciences, San Jose, CA, USA).

PMPs, defined as having a diameter <1 μm and $CD61^+$, was also analyzed with flow cytometry. FITC-conjugated mouse IgG (isotype) was used as the negative control. PMPs from the same volume of plasma from the hypertensive or control rats were compared. Using the same method, PMPs produced by platelets with or without thrombin stimulation *in vitro* were also detected.

Laser scattering electrophoresis (LSE) was used to directly detect the concentration of MPs or PMPs in plasma or suspension. The LSE chamber was washed 3 times with pure water and then with PBS to remove the residual nanoparticles. The standard sample was used to determine the particle size. Five milliliter aliquots of diluted samples were used to detect the size and concentration of the particles.

Stimulation of ECs with platelets, MPs, MP-poor plasma, and PMPs

Platelets, MPs, and PMPs were quantified with BD Trucount Tubes (20,000/ml) by flow cytometry. ECs were incubated with platelets (10^7 and 10^5/ml), MPs ($10^9$and 10^7/ml), MP-poor plasma (10 and 5% by volume), or PMPs (10^9/ml) for up to 48 h at 37°C with 5% CO_2.

Incubation of platelets and PMPs with ECs and the fluorescence assays

To analyze the adhesion of PMPs or platelets to ECs, PMPs and platelets were labeled with PKH67, a general cell membrane marker (PKH67 Fluorescent Cell Linker Kits; MilliporeSigma, Billerica, MA, USA), and then incubated with ECs for 1 h. After 3 rinses, fluorescence images were acquired by confocal microscopy (LV1000; Olympus, Tokyo, Japan).

FISH analysis

After PMPs incubated with ECs for 12 h, ECs were fixed with 4% paraformaldehyde overnight and washed 3 times in PBS. To block endogenous peroxide activity, the ECs were treated with 0.3% H_2O_2 before acetylation in acetic anhydride-triethanolamine, and washed in 2× saline sodium citrate (SSC) and PBS before permeabilization with proteinase K (5 μg/ml). ECs then were hybridized with miR-142-3p biotinylated probe (5′ biotin-TCCATAAAGTAGGAAACACTACA-3′) (Shanghai GenePharma, Shanghai, China) (200 nM) overnight at 56°C. After posthybridization washes in 5 times SSC at room temperature, 50% formamide/1 time SSC/0.1% Tween 20 at the

hybridization temperature, and 0.2 times SSC at room temperature, FISH signals were amplified by Tyramide SuperBoost Kits followed with an AlexaFluor Tyramide Kit (B40933; Thermo Fisher Scientific) and photographed on a microscope (DP70; Olympus).

microRNA array analysis

Total RNA was harvested with Trizol (Thermo Fisher Scientific) and the miRNeasy Mini Kit (Qiagen, Germantown, MD, USA) according to the manufacturers' instructions. After the RNA quantity was measured with a NanoDrop 1000, the samples were labeled using the miRcury/Hy3/Hy5 Power Labeling Kit and hybridized on a miRcury LNA Array (v.18.0). Following the washing steps, the slides were scanned with the Axon GenePix 4000B Microarray Scanner.

Scanned images were then imported into GenePix Pro 6.0 software (Axon Technologies, Scottsdale, AZ, USA) for grid alignment and data extraction. Replicated miRs were averaged, and miRs with intensities $\geq$30 in all samples were used to calculate the normalization factor. Expression data were normalized by the median normalization method.

Small interfering RNA transfection

For the RNA interference experiment, ECs were transfected with 100 nM of rno-miR-142-3p mimics, rno-miR-142-3p inhibitor, Bcl-2-associated transcription factor (BCLAF)1 small interfering RNA (siRNA) or control nonsilencing siRNA (Shanghai GenePharma) for 8 h with Lipofectamine 2000 in Opti-MEM (both from Thermo Fisher Scientific) according to the manufacturer's instructions. The sequences of the siRNA oligos are listed in Supplemental Table 1.

Real-time quantitative PCR

Total RNA was isolated with Trizol Reagent. For the isolation of RNAs from PMPs, *Caenorhabditis elegans* miR-39 (cel-miR-39) was added to each sample as a spike-in control. The isolated RNA was reverse transcribed into cDNA with the Moloney murine leukemia virus real-time system using the reverse transcribe primer for miRs (Shanghai GenePharma) or oligo-dT for mRNA. Real-time quantitative PCR (qPCR) was performed with SYBR Green Supermix (Takara, Kyoto, Japan), and the levels of precursor and mature miRs were normalized against the control U6 snRNA or cel-miR-39. For comparison of miRs between ECs and platelets which are 2 different kinds of cells, the nematode source of exogenous cel-miR-39 was introduced by the $2^{-\Delta\Delta}C_t$ value method. *C. elegans* cel-miR-39 does not overlap with mammalian miRs completely. qPCR was performed and analyzed in a Mini-Opticon Real-Time PCR System (Bio-Rad, Hercules, CA, USA), with the QuantiTect SYBR green PCR Kit (Qiagen). Specific primer sequences are listed in Supplemental Table 2.

Western blot analysis

Western blot analysis was performed with antibodies directed against BCLAF1 (1:300; Santa Cruz Biotechnology, Dallas, TX, USA) and B-cell lymphoma-2–associated (Bax; 1:1000), B-cell lymphoma (BCL)-2 (1:1000), and β-tubulin (1:1000; all from Cell Signaling Technology, Danvers, MA, USA). After incubation with alkaline phosphatase–conjugated secondary antibodies (1:1000; Jackson ImmunoResearch Laboratories, West Grove, PA, USA), the signals were visualized with nitroblue tetrazolium/bromo-chloro-indolyl phosphate (Bio Basic, Markham, ON, Canada) and quantified with Quantity One software (Bio-Rad).

Dual-luciferase reporter assay

The conserved miR-142-3p-binding sequences in the 3′ UTR of BCLAF1 and mutated target-site sequences were both obtained by gene synthesis and then inserted downstream of the luciferase reporter gene (psiCheck-2; Promega, Madison, WI, USA). To determine the suppression efficiency of miR-142-3p, HEK-293T cells were transfected with the reporter plasmid or the mutated vectors, together with miR-142-3p mimics or a negative control. After 24 or 48 h, firefly and *Renilla* luciferase activities were consecutively measured using the dual-luciferase reporter assay system (Promega).

Cell proliferation and apoptosis assay

EC proliferation *in vivo* was analyzed using the *In Situ* Cell Proliferation Kit (Fluos; Roche, Basel, Switzerland). Twenty-four hours before harvest, bromodeoxyuridine (BrdU; MilliporeSigma) was intraperitoneally injected into the rats (200 mg/kg). The thoracic aortae (0.7 cm) were isolated, fixed, dehydrated with isopentane for 24 h, fixed with 70% ethanol in 50 mM glycine buffer, digested with 0.05% trypsin solution, denatured with 2 M HCl, and labeled with anti-BrdU antibody (1:800; MilliporeSigma), followed by a fluorescent secondary antibody (1:1000; Cell Signaling Technology). The nuclei were stained with DAPI. Blood vessels were dissected longitudinally, and flattened between coverslips. Five fields in each vessel were selected, and EC proliferation was visualized using an FV1000 laser scanning confocal microscope (Olympus). The ratio of proliferating ECs marked by BrdU to total ECs marked by DAPI was calculated and normalized with the average of all control groups.

EC proliferation *in vitro* was analyzed with a colorimetric BrdU kit (Roche). Eight hours before detection, the BrdU labeling reagent was added to the culture medium (1:1000). ECs were fixed and labeled according to the manufacturer's instructions. Absorbance was measured at a wavelength of 450 nm and a reference wavelength of 630 nm in an ELISA Plate Reader (680; Bio-Rad).

The Cleaved Caspase-3 ELISA kit (Cell Signaling Technology) was used to assess EC apoptosis *in vivo* and *in vitro*, according to the manufacturer's instructions. ECs were treated with lysis buffer (with 1 mM PMSF freshly added) on ice. Lysates were transferred to appropriate tubes and then centrifuged for 10 min at 14,000 rpm and 4°C. Absorbance was measured at 450 nm in an ELISA Plate Reader.

Ingenuity Pathway Analysis

The possible biologic processes and the functional classifications in which the target genes of miR-142-3p may be involved were obtained by Ingenuity Pathway Analysis (IPA) software (Qiagen) (*https://www.qiagenbioinformatics.com/products/ingenuity-pathway-analysis*, content version: 39480507/). IPA integrates the available knowledge on genes, drugs, chemicals, protein families, processes, and pathways, based on the interactions and functions derived from the Ingenuity Pathways Knowledge Database Literature. IPA is used to understand the complex biologic and chemical systems at the core of life science research based on lectures or predicated analysis (17).

Statistical analysis

Each experiment was performed at least 4 times, and all values are expressed as means ± SD. One-way ANOVA was used to compare the results between 2 groups. Values of $P < 0.05$ were statistically significant.

RESULTS

Hypertension increased the EC proliferation and the number of circulating PMPs

One week after surgery, systolic blood pressure (SBP) and diastolic blood pressure (DBP) were measured. As shown in **Fig. 1*A***, the SBP and DBP of hypertensive rats were significantly increased compared with those of the sham-treated control rats (SBP 151.30 ± 10.15 mmHg *vs.* 90.95 ± 4.93 mmHg and DBP 93.24 ± 8.19 mmHg *vs.* 62.35 ± 5.06 mmHg). Meanwhile, the body weight of the hypertensive rats was significantly lower than that of the control rats (Fig. 1*B*). EC proliferation was increased in the thoracic aorta as detected by the BrdU assay (Fig. 1*C*).

To detect platelet activation in the hypertension model, CD62p (platelet activation marker) and CD61 (platelet marker) were detected *via* flow cytometry. The double-positive ($CD61^+/CD62P^+$) dots in the upright quadrant represented the active platelets, and the platelet activation rate of the hypertensive rats was increased from ~9.31% to ~15.02% compared with that of the sham-treated control rats (Fig. 1*D*). In addition, compared with the sham-treated control, the number of circulating MPs in plasma of hypertensive rats, which was directly analyzed with LSE without centrifugation, also increased significantly (Fig. 1*E*).

Furthermore, PMPs, which are the main part of circulating MPs and partially reflect the activation of platelets, were detected (18). Flow cytometry combined with platelet marker showed that there is no significant difference between the ratio of PMPs to MPs in hypertensive and control groups (Fig. 1*F*). The PMP counts in the same volume of plasma from hypertensive and control group were compared. Negative control was used to define the positive "M" region (5% confidence intervals). After normalized with the average of control groups, the results showed that, compared with the control group, hypertension increased the plasma concentration of PMPs (Fig. 1*G*).

These results suggested that EC dysfunction and platelet activation occur simultaneously in hypertensive rat models; therefore, we next explored how the activated platelets affect EC proliferation.

MPs from hypertensive rats enhanced EC proliferation

We first detected the effect of different plasma components from the hypertensive rat model on EC proliferation.

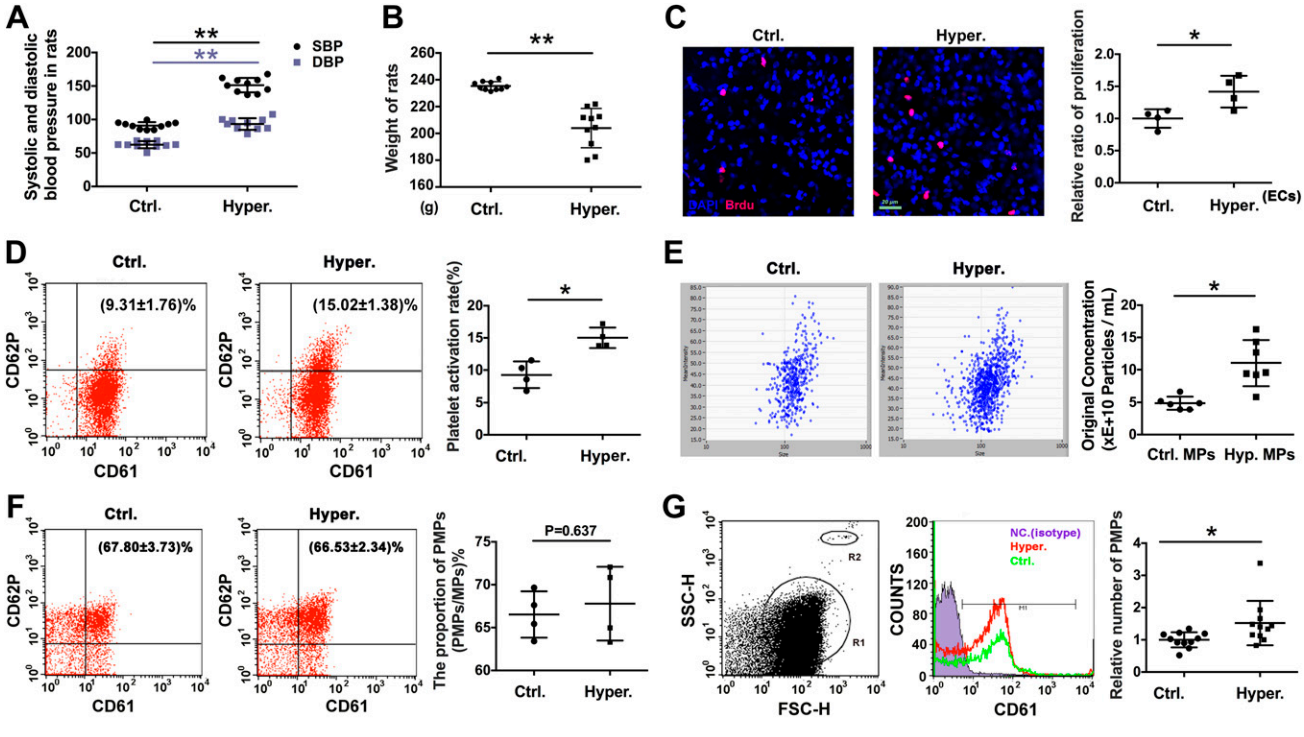

Figure 1. Hypertension increased the proliferation of ECs and increased the number of PMPs. *A*) SBP and DBP of hypertensive and normotensive rats 1 wk after abdominal aortic coarctation surgery and sham surgery, respectively ($n = 10$/group). *B*) One week after surgery, body weight was recorded in the surgery and control groups ($n = 10$/group). *C*) EC proliferation in the thoracic aorta was detected with BrdU *in situ* immunofluorescence staining (red) in hypertensive and control rats ($n = 4$/group). Scale bar, 20 μm. *D*) The activation rate of platelets was assessed with flow cytometry, which detected CD61 (platelet marker) and CD62p (platelet activation marker) labeling ($n = 4$ independent experiments). *E*) Using LSE and Brownian motion video microscopy, the concentrations of MPs in plasma from the hypertensive and control rats without volumetric ultracentrifugation were compared ($n = 6$/group). *F*) The MPs were labeled with platelet marker, and the PMP:MP ratio in the hypertensive group and the control group was analyzed by flow cytometry ($n = 4$/group). *G*) Circulating MPs (gate R1) were extracted from hypertensive rats and normotensive rats; their sizes were defined with 2.5 μm beads (gate R2), and the number of PMPs was determined by CD61 labeling combined with flow cytometry ($n = 11$/group). Column scatter showing the fold change relative to the control. Values are means ± SD. $^*P < 0.05$, $^{**}P < 0.01$.

Platelets, circulating MPs, and MP-poor plasma from the hypertensive and sham-treated animal models were isolated as shown in **Fig. 2*A***. Figure 2*B* shows that stimulation of ECs with M199 medium containing 5 or 10% MP-poor plasma did not alter EC proliferation. In addition, stimulation of ECs with platelets at different concentrations (10^7 and 10^5/ml) had no significant effect on EC proliferation (Fig. 2*C*).

However, EC proliferation was significantly upregulated after stimulation with MPs (both 10^9 and 10^7/ml) (Fig. 2*D*), which suggested that MPs play significant roles in EC dysfunction in hypertension. Because it has been reported that most of the MPs in the blood are derived from platelets (19), we further detected the role of PMPs in EC proliferation and the potential molecular mechanism *in vitro*.

Thrombin was increased in hypertensive rats and induced PMP release

Thrombin is a crucial inducer of platelet activation and has been reported to be significantly increased in the vessel wall of spontaneously hypertensive rats (20). Thrombin content in the same amount of plasma was significantly

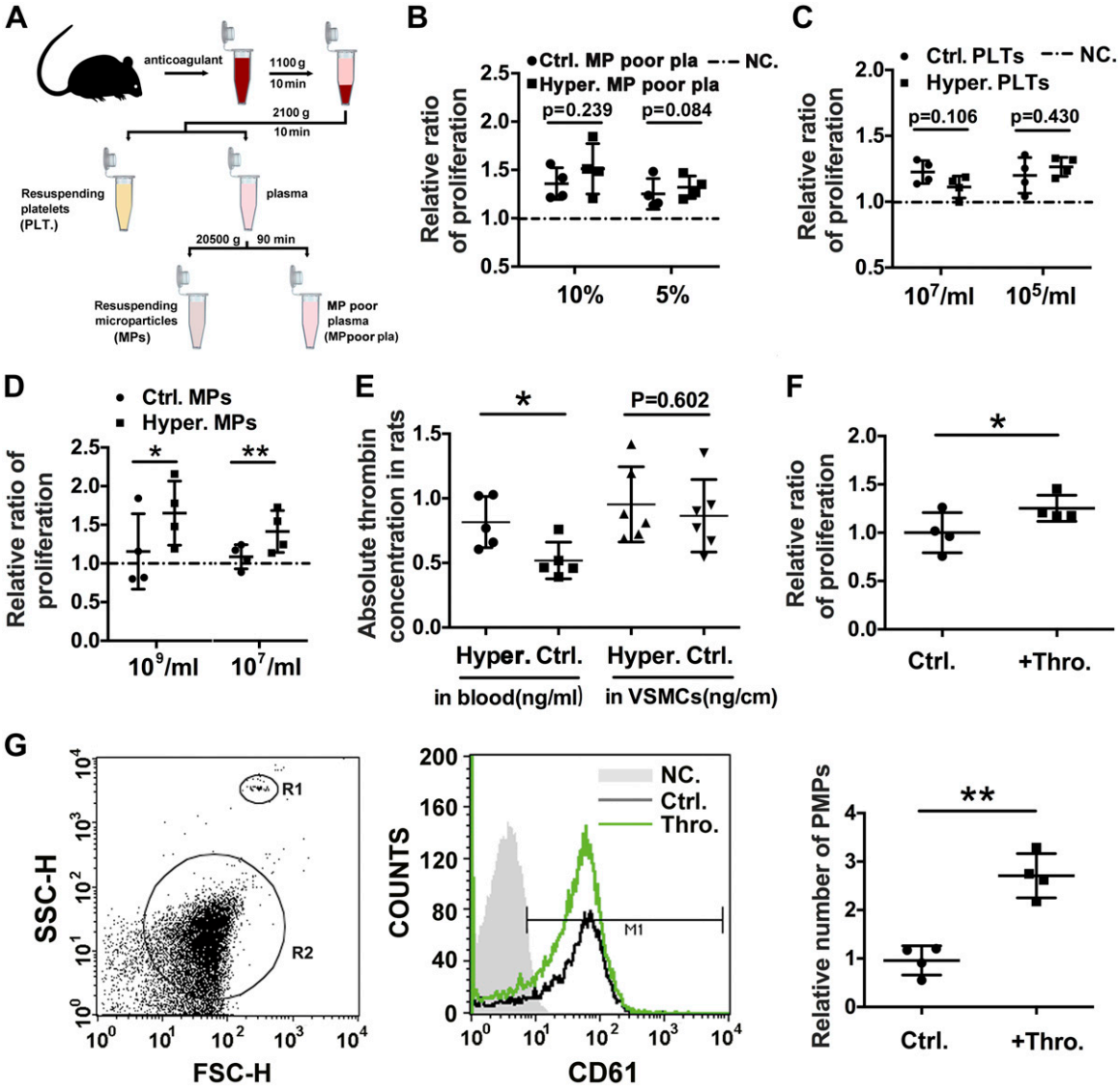

Figure 2. MPs from hypertensive rats enhanced EC proliferation. *A*) The flow chart shows the isolation of platelets, circulating MPs and MP-poor plasma from the hypertensive and sham-surgery animal models. *B–D*) Ten and 5% MP-poor plasma (*B*), 10^7 and 10^5/ml platelets (PLTs) (*C*), and 10^9 and 10^7/ml MPs (*D*) from the hypertensive and control rats were added to ECs for 48 h, and then, EC proliferation was examined with a BrdU assay ($n = 4$/group). *E*) The absolute thrombin concentration in plasma and the thoracic aorta of hypertensive and control rats was detected with ELISA ($n = 4$/group). *F*) PMPs were collected by centrifugation after the same number of platelets were stimulated with 0.1 U/ml thrombin for 1 h; then, they were applied to stimulate ECs for 1 h. EC proliferation was detected by a BrdU assay ($n = 4$/group). *G*) After platelets were stimulated with 0.1 U/ml thrombin for 1 h, PMPs (gate R2) from hypertensive rats and normotensive controls were extracted, and their sizes were defined with 2.5 μm beads (gate R1). The number of PMPs was determined by CD61 labeling, which was assessed with flow cytometry ($n = 4$ independent experiments). Column scatter shows the fold change relative to the control. Values are means ± SD. $^*P < 0.05$, $^{**}P < 0.01$.

up-regulated in the renal hypertensive rats compared with the sham-treated control rats, but it was unchanged in the same length of thoracic aorta (Fig. 2*E*).

After thrombin stimulation *in vitro*, the platelets produced 2.71 times more PMPs than those of the control group (Fig. 2*G*). The collected PMPs released by the same number of platelets, stimulated with thrombin, induced a remarkable increase in EC proliferation (Fig. 2*F*). These results suggest that circulating thrombin is an important platelet activator in hypertension that induces the release of PMPs, which may subsequently increase EC proliferation. The mechanism by which PMPs modulate EC proliferation was further explored.

The expression of miR-142-3p was higher in PMPs and could enter ECs

Platelets contain numerous miRs; however, the miR expression profile in PMPs and the role of miRs in abnormally proliferating ECs in hypertension are still unclear. **Table 1** shows the top 15 most abundantly expressed miRs in platelets, as determined with a microRNA array, and miR-142-3p, ranked number 1. Using cel-miR-39 as a spike-in control/external reference, the expression of miR-142-3p in the platelets and ECs was compared by the $2^{-\Delta\Delta}$ C_t method. **Figure 3*A*** shows that the relative expression of miR-142-3p is ~96.8 times higher in platelets than in ECs. Moreover, in PMPs isolated from the same blood volume, the expression of miR-142-3p was 3.24 times higher in the sample from hypertensive rats than in the sample from control rats (Fig. 3*B*).

Furthermore, 0.1 U/ml thrombin remarkably increased the expression of miR-142-3p in both platelets (Fig. 3*C*) and PMPs (Fig. 3*D*). The significant enrichment of miR-142-3p in platelets and PMPs provided a useful monitoring molecule with which to investigate the communication and information delivery from platelets to ECs.

ECs were then stimulated with platelets or PMPs to detect whether miR-142-3p could be transferred into ECs. After incubation, PMPs increased the expression of miR-142-3p in ECs by 5.25-fold (Fig. 3*E*), whereas stimulation with activated platelets did not cause a significant change in miR-142-3p expression (Fig. 3*F*). Because there was a slight (not significant) increase in the expression of miR-142-3p in ECs treated with activated platelets, we sought to detect the interaction of platelets or PMPs with ECs by morphologic analysis. Immunofluorescence showed that after incubation for 1 h, PMPs were markedly enriched around ECs (Fig. 3*G*). A small release of PMPs from activated platelets was also detected, and the locally released PMPs may directly adhere to the ECs.

FISH also confirmed the *in situ* expression of miR-142-3p in ECs stimulated with PMPs. Figure 3*H* showed that after stimulation with PMPs for 12 h, cytoplasmic miR-142-3p in ECs increased significantly.

The results show that PMPs are important vehicles that transfer platelet-specific miR to ECs. We then explored the role and molecular mechanism of PMP-delivered miR-142-3p in EC proliferation.

TABLE 1. *The top 15 most abundantly expressed miRs in platelets*

miR	Signal intensity
miR-142-3p	39,116.0
miR-22-3p	28,200.5
miR-126-3p	21,121.5
miR-26b-5p	18,193.5
miR-16-5p	14,375.0
miR-23a-3p	11,858.5
miR-23b-3p	11,655.0
miR-142-5p	11,192.5
miR-15a-5p	10,674.0
miR-191-5p	10,386.0
miR-103a-3p	9,685.0
miR-20a-5p	8,609.5
miR-24-3p	8,556.0
miR-223-3p	8,122.5
miR-15b-5p	7,433.5

miR-142-3p promoted EC proliferation *via* BCLAF1

To detect the potential mechanisms involved in the effect of platelet-derived miR-142-3p on EC proliferation or apoptosis, we analyzed the potential target genes of miR-142-3p using IPA bioinformatics software. The grow tool was used to predicate all the target genes of miR-142-3p, and then the function analysis tool of the software was used to obtain the molecules related to cell proliferation and apoptosis. IPA revealed that there are 160 downstream target molecules that interact with miR-142-3p, including 65 molecules that are associated with either proliferation or apoptosis (**Fig. 4*A*** expressed in the middle pink regions), among which 40 molecules are related to both proliferation and apoptosis (shown as a green icon).

Using the high predicted standard in IPA software, in which the miRs and mRNA have conserved pairing sites and the confidence evaluation was less than −0.4, only 4 high predictors were identified (**Table 2**). TargetScan, miRanda, and PicTar predicted the consequential pairing of miR-142-3p to the BCLAF1 3′UTR (Fig. 4*B*). miR-142-3p mimics and inhibitors were then transferred to ECs to detect the effect of miR-142-3p on EC proliferation.

The results showed that EC proliferation was significantly up-regulated in the miR-142-3p mimics-transferred group, whereas the miR-142-3p inhibitor had no significant effect on EC proliferation (Fig. 4*C*). miR-142-3p mimics also decreased the expression of the target molecule BCLAF1 in ECs, which was not changed by the miR-142-3p inhibitor (Fig. 4*D*). The lower effect of the inhibitor may be related to the low basal level of miR-142-3p in ECs.

Using the dual-luciferase reporter assay, we confirmed whether miR-142-3p targets the 3′-UTR of BCLAF1 and leads to translational repression. We observed a significant down-regulation of luciferase activity upon coincubation with miR-142-3p mimics and wild-type BCLAF1 3′UTR for both 24 and 48 h (Fig. 4*E*, *F*). Moreover, the decrease in luciferase activity was reversed when miR-142-3p was cotransfected with the plasmid containing the mutated binding site in the BCLAF1 3′UTR.

Together, these results confirmed that BCLAF1 is the target of miR-142-3p and that miR-142-3p represses BCLAF1

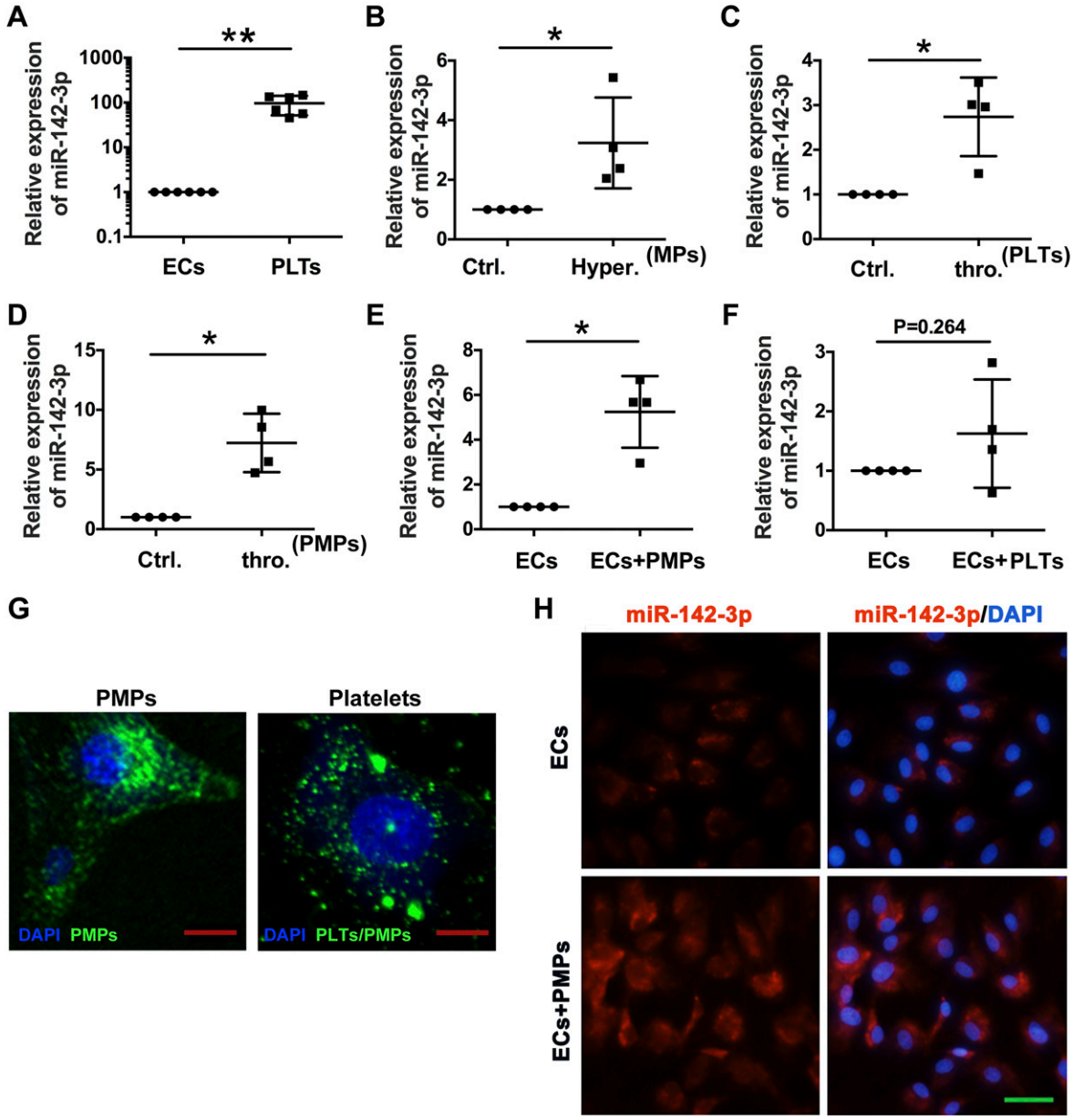

Figure 3. miR-142-3p was more highly expressed in PMPs and could enter ECs. *A*) The relative expression of miR-142-3p in the platelets and ECs was compared by qPCR using the $2^{-\Delta\Delta}C_t$ method ($n = 6$/group). *B*) The expression of miR-142-3p in MPs from the same volume of blood from hypertensive and control rats was measured by qPCR ($n = 4$/group). *C, D*) The expression of miR-142-3p in activated platelets (*C*) and secreted PMPs (*D*) was analyzed after stimulation with 0.1 U/ml thrombin for 1 h by qPCR ($n = 4$/group). *E, F*) The expression of miR-142-3p in ECs was measured after incubation with PMPs (*E*) or PLTs (*F*) by qPCR ($n = 4$/group). *G*) PMPs and PLTs were incubated with ECs for 1 h and rinsed. Green fluorescence shows the membranes of PMPs and PLTs, which were labeled with PKH67 fluorescent cell linker; blue fluorescence shows the EC nuclei, which were labeled with DAPI. Scale bars, 5 μm. *H*) miR-142-3p is detected with FISH in ECs incubated with PMPs for 12 h. miR-142-3p was labeled with biotin and amplified by tyramide signal amplification kits following with a red fluorescence tyramide kit; EC nuclei were labeled with DAPI (blue fluorescence). Column scatter showing the fold change relative to the control. Values are means ± SD. $^*P < 0.05$, $^{**}P < 0.01$. Scale bar, 20 μm.

expression. The results also suggested that PMP-delivered miR-142-3p may induce EC proliferation *via* BCLAF1.

BCLAF1 promoted EC proliferation *via* BCL2 and Bax

To explore the effect of BCLAF1 on EC proliferation and the downstream genes related to BCLAF1, a BCLAF1-specific small interfering RNA was applied. Three interference fragments were synthesized, and their effects on the mRNA and protein levels of BCLAF1 were detected (**Fig. 5*B, C***). Based on IPA, 12 genes related to BCLAF1, as well as both cell proliferation and apoptosis, were revealed (Fig. 5*A*). Six target genes, mouse double minute (MDM)-2 homolog, BCL2, tumor protein (TP)-53, cyclin-D1, BAX, and Wilms tumor suppressor-1 associated protein, were investigated as the BCLAF1 protein was reported to interact with their DNA (PD). qPCR showed that

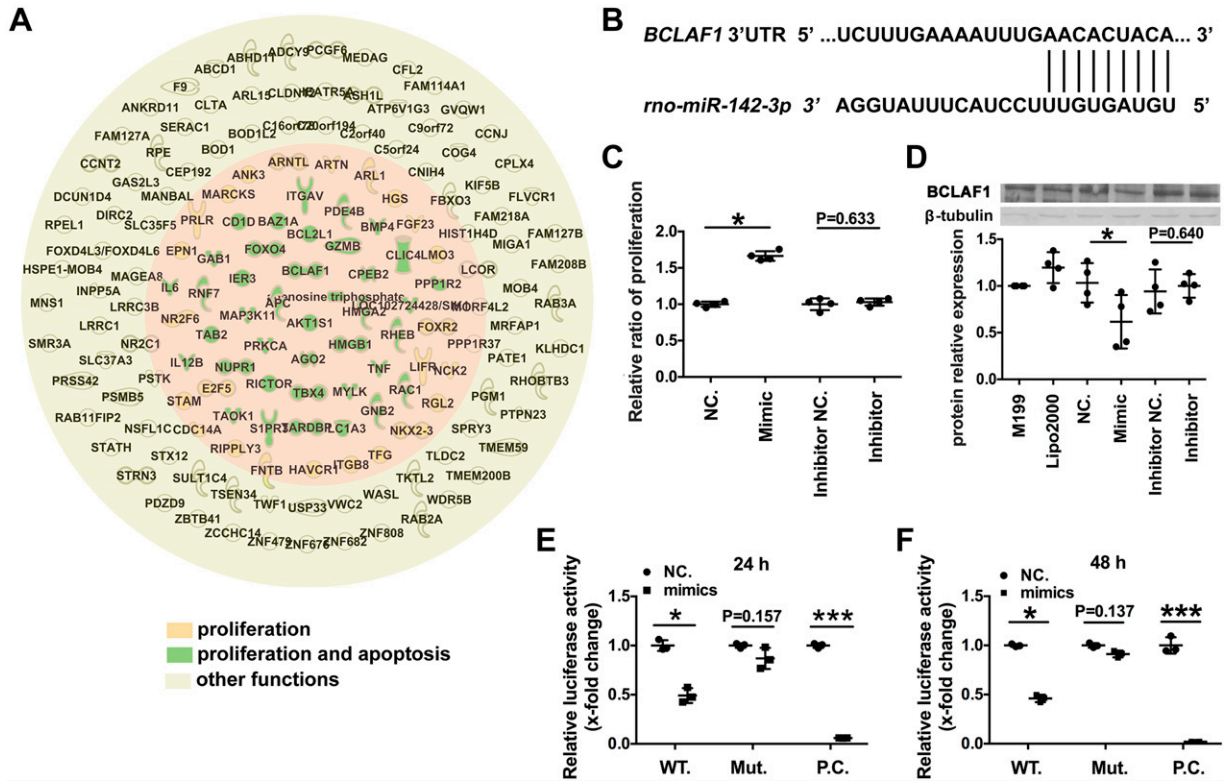

Figure 4. miR-142-3p promoted EC proliferation *via* BCLAF1. *A*) The potential target genes of miR-142-3p were predicted with IPA software. A total of 160 downstream target molecules that directly interact with miR-142-3p were screened by IPA. The 65 target molecules associated with either proliferation or apoptosis are shown in the pink regions. The green icon indicates the 40 target molecules related to both proliferation and apoptosis. *B*) Sequence alignment between rno-miR-142-3p and its putative binding sites in the 3′-UTR of rat BCLAF1 mRNA. *C*) ECs were transfected with miR-142-3p mimic or miR-142-3p inhibitor, and EC proliferation was assessed with BrdU ELISA ($n = 4$/group). *D*) The expression level of BCLAF1 in ECs that were transfected with miR-142-3p mimic or inhibitor was detected by Western blot after 48 h ($n = 4$/group). *E, F*) Luciferase activities in HEK-293T cells expressing wild-type BCLAF1 3′-UTRs (WT), mutant BCLAF1 3′-UTRs (MUT) and positive control (PC) were measured consecutively using the dual-luciferase reporter assay system 24 (*E*) and 48 (*E*) h after all groups were transfected with negative control (NC) or miR-142-3p mimics. Column scatter showing the fold change relative to the control. Values are means ± SD. $^*P < 0.05$, $^{***}P < 0.001$.

MDM2, BCL2, TP53, and BAX were up-regulated after BCLAF1 siRNA transfection (Fig. 5*D*).

As BCL2 and Bax are particularly important in cardiovascular disease (21), we verified their protein expression levels and revealed that BCLAF1 siRNA transfection increased their protein expression (Fig. 5*E*), which was consistent with the mRNA changes. Furthermore, EC proliferation was significantly up-regulated after BCLAF1 siRNA transfection (Fig. 5*F*). Together, these results suggest that PMP-delivered miR-142-3p may induce EC proliferation *via* BCLAF1 and that genes downstream of BCLAF1, such as BCL2 and Bax, may be involved in this process.

DISCUSSION

PMPs were first identified during blood coagulation research in 1967 and were termed as platelet dust (22). We now know that PMPs contain abundant bioactive proteins and genetic materials and transfer these bioactive molecules from platelets to recipient cells in the circulatory system. The present research uncovered that PMPs increase EC proliferation in hypertension and demonstrated that miR-142-3p was highly expressed in PMPs and could be delivered into ECs, which effectively suppressed BCLAF1 expression and increased EC proliferation (**Fig. 6**).

EC dysfunction, such as reduced NO bioavailability (23) and abnormal oxidative stress (24), apoptosis, and proliferation (25), plays important roles in vascular remodeling in hypertension. As early as 1977, Schwartz and Benditt (1) reported that after renal hypertension for 2–3 wk, the rate of EC replication rises 10-fold. This increase may represent an increase in EC turnover, which probably represents, at least in part, a proliferative response to cover the expanded luminal surface of the dilated vessel (26). However, the molecular mechanisms involved in this process remain unclear. Nishimura *et al.* (27)

TABLE 2. *Four high predictors were identified with IPA*

Symbol	Location	Type
AGO2	Cytoplasm	Translation regulator
BCL2L1	Cytoplasm	Other
BCLAF1	Nucleus	Transcription regulator
LIFR	Plasma membrane	Transmembrane receptor

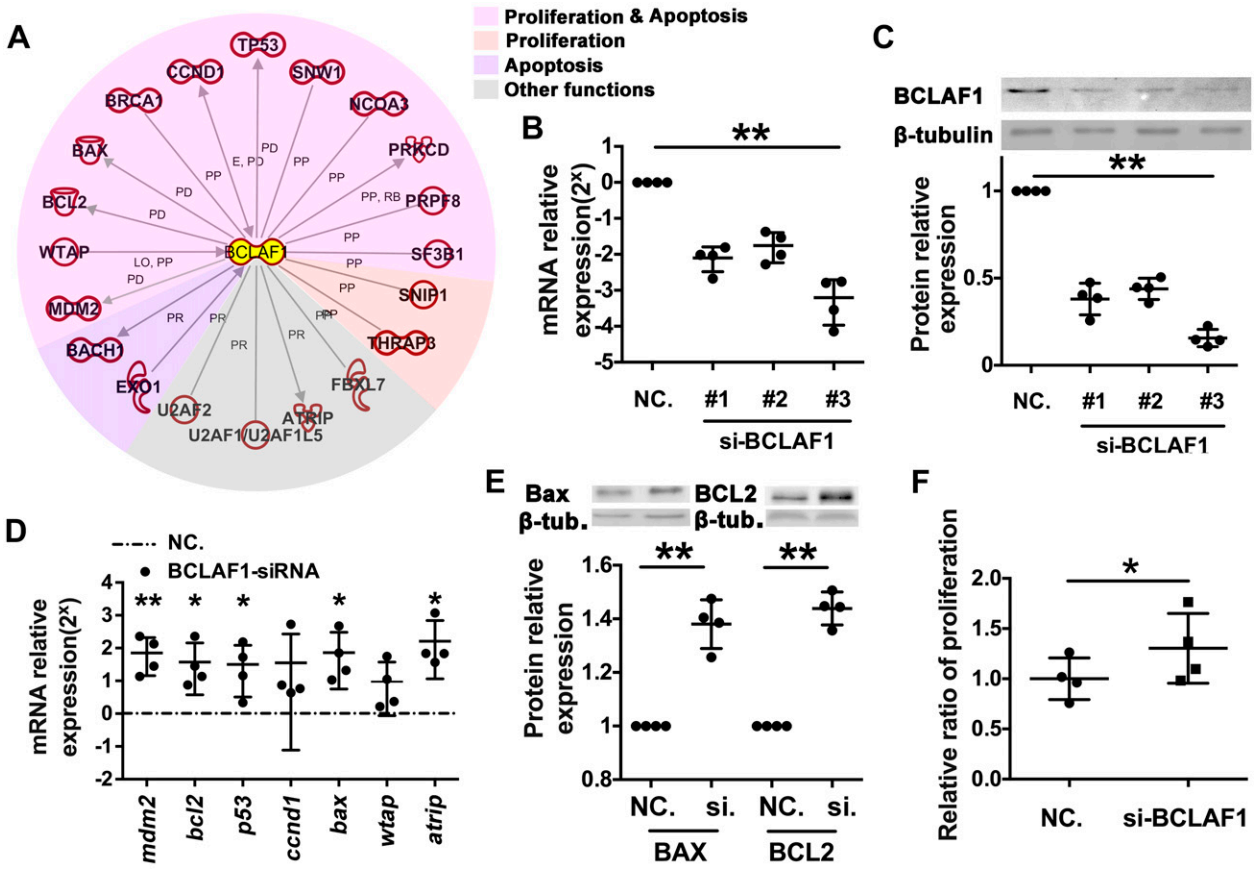

Figure 5. BCLAF1 promoted EC proliferation *via* BCL2 and Bax. *A*) The molecules that interact with BCLAF1 were predicted using IPA software and classified by function. *B*, *C*) The expression level of BCLAF1 in ECs that were transfected with 3 BCLAF1 siRNA fragments was detected by qPCR (*B*) and Western blot (*C*) after 48 h ($n = 4$/group). *D*, *E*) The expression level of the molecules interacting with BCLAF1 was assessed by qPCR (*D*) and Western blot (*E*) 48 h after the ECs were transfected with BCLAF1 siRNA #3. *F*) EC proliferation was detected by BrdU ELISA 48 h after ECs were transfected with BCLAF1 siRNA #3 ($n = 4$/group). Column scatter showing the fold change relative to the control. Values are means ± SD. $^*P < 0.05$, $^{**}P < 0.01$.

reported that high cycle stress promotes the proliferation of ECs, which participates in hypertension-induced pathologic changes. Our previous experiments also reported that vascular smooth muscle cells secrete miR-27a and modulate the proliferation of ECs in hypertension (26). These findings indicate that both direct sensing of stress and the interaction between cells are involved in the promotion of EC proliferation in hypertension.

EC apoptosis also plays important roles in pathologic EC turnover in hypertension (28). In the present experiments, we also detected the effect of different plasma components on EC apoptosis. The results of EC apoptosis were different compared to those of EC proliferation, showing that MP-poor plasma from hypertensive rats increases EC apoptosis, whereas MPs decrease EC apoptosis (Supplemental Fig. 1*A*, *D*). At present, the impact of MPs on EC apoptosis is still not clear. Sheu *et al.* (29) showed that MPs from patients with lung cancer decrease c-caspase3 in a rat model of critical limb ischemia, whereas in chronic cerebral ischemia, MPs deliver proapoptotic signals to cultured ECs (30). In the cardiovascular system, MPs can promote endothelial dysfunction and lead to the development of cardiovascular diseases (31). Our results show that platelets in hypertensive rats inhibit EC apoptosis (Supplemental Fig. 1*C*), which is consistent with the results of Jiang *et al.* (5). In their opinion, platelets can be phagocytosed by ECs, and the phagocytosed platelets could suppress endothelial apoptosis and promote cell viability. In general, our results revealed that the components of hypertensive rat blood induce EC dysfunction and that PMPs are involved in the regulation of EC proliferation, whereas EC apoptosis may be more complicated and may involve more factors.

Increasing evidence has shown that many factors in the blood affect EC function, including growth factors (32), inflammatory factors (33), and circulating MPs (34). Our present experiments explored the effect of PMPs released from activated platelets. Our present results suggest that PMPs are important vehicles that deliver miRs into ECs.

miRs are the most important molecules involved in cellular communication and can be transferred between cells in various ways. For example, exosomes, which are vehicles with a relatively small diameter (40–100 nm), deliver miR-214 to regulate tissue growth factors (35). In addition, argonaute2 can bind with miRs and facilitate the direct transfer of miRs to another cell (36). Circulating MPs act as transport vehicles for numerous specific miRs. It has been reported that miR-223, which was also detected in our microRNA array as an abundant miR in platelets (ranked 14th), can be delivered from platelets into ECs *via*